Available online at www.sciencedirect.com

SciVerse ScienceDirect

Scripta Materialia 66 (2012) 919–922

Scripta MATERIALIA

www.elsevier.com/locate/scriptamat

# Size-dependent rupture strain of elastically stretchable metal conductors

O. Graudejus,[a,*] Zheng Jia,[b] Teng Li[b,*] and S. Wagner[c]

[a]*Department of Chemistry and Biochemistry, Center for Adaptive Neural Systems, Arizona State University, Tempe, AZ 85287, USA*

[b]*Department of Mechanical Engineering, Maryland NanoCenter, University of Maryland, College Park, MD 20742, USA*

[c]*Department of Electrical Engineering, Princeton Institute for the Science and Technology of Materials, Princeton University, Princeton, NJ 08544, USA*

Received 14 November 2011; revised 17 February 2012; accepted 19 February 2012
Available online 25 February 2012

Experiments show that the rupture strain of gold conductors on elastomers decreases for conductors that are long and narrow. Rupture is caused by the irreversible coalescence of microcracks into one long crack. A mechanics model identifies a critical crack length $\ell_{cr}$ above which the long crack propagates across the entire conductor width. $\ell_{cr}$ depends on the fracture toughness of the gold film and the width of the conductor. The model provides guidance for the design of highly stretchable conductors.


*Keywords:* Thin films; Rupture strain; Stretchable conductors; Flexible electronics

Elastically stretchable conductors have been explored for biomedical applications [1–3], as dielectric elastomer actuators [4], and as stretchable electronics [5,6]. A class of highly stretchable conductors consists of gold films on substrates of the elastomer polydimethylsiloxane (PDMS). Depending on the fabrication conditions, these gold films can adopt three morphologies: microcracked, buckled, and smooth [7]. We are particularly interested in microcracked films, because they can be elastically stretched to, and relax from, large strains while remaining electrically conductive [8]. For example, 40 μm wide and 5 mm long microcracked gold conductors on 300 μm thick PDMS can be stretched reversibly to about 50% uniaxial strain [9]. However, at 90% uniaxial strain electrical conductance is lost because at one or a few locations microcracks coalesce to form one long crack that severs the entire conductor. The parameters that determine the formation of such long cracks have not been understood. Here we show experimentally that the rupture strain $\varepsilon_r$ increases with the width and decreases with the length of the conductor, and present a mechanics model that explains this size dependence of the rupture strain.

75 nm thick microcracked gold films on a 2–3 nm chromium adhesion layer are deposited at <65 °C substrate temperature on 300 μm thick PDMS. The as-deposited film contains 0.5–2 μm long randomly distributed microcracks, which delineate a stretchable gold network. The gold film is formed into $L = 5$ and 20 mm long and $W = 6$, 25, 45, and 95 μm wide conductors by lithography and wet etching [7,9] (Fig. 1a). The distribution of microcracks within these conductors is homogeneous, without appreciable edge effects, because the microcracks in the gold film are produced during deposition. Figure 1 shows scanning electron micrographs of a microcracked gold film before stretching (Fig. 1b), an optical micrograph of a 95 μm wide conductor during stretching at 10% strain (Fig. 1c), and an electron micrograph after stretching to a maximum strain of ~90% (Fig. 1d). The electron micrograph after stretching clearly shows the coalescence of microcracks perpendicular to the stretching direction. The electron micrograph and optical micrograph images show that the microcracks coalesce homogeneously throughout the conductor, perpendicular to the stretching direction. Patterned conductors are stretched in steps of 0.1% every 3 s up to a designated maximum strain, and then relaxed at the same rate, while the electrical resistance $R$ is recorded. After 3–5 cycles the designated maximum strain is increased by 10%, and the gold conductor is stretched and relaxed

* Corresponding authors. E-mail addresses: oliver.graudejus@asu.edu; lit@umd.edu

1359-6462/$ - see front matter © 2012 Acta Materialia Inc. Published by Elsevier Ltd. All rights reserved.
doi:10.1016/j.scriptamat.2012.02.034

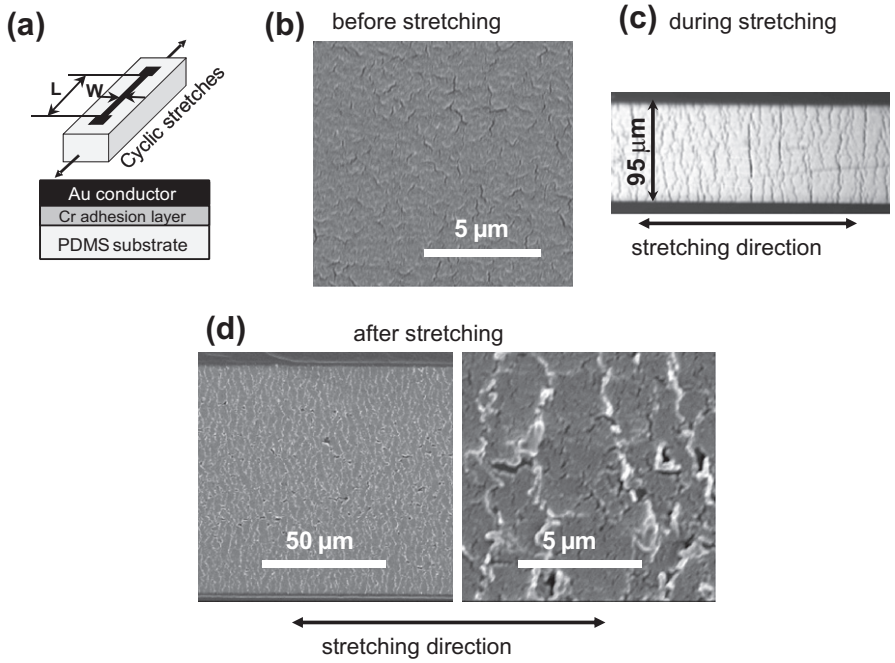


**Figure 1.** (a) Schematic and cross-sectional view (not to scale) of a gold conductor on a PDMS substrate. (b) SEM image of the microcrack morphology in the gold conductor before stretching. (c) Optical micrograph of a microcracked conductor during stretching (width 95 μm, 10% strain, $R = 230\ \Omega$). (d) SEM image after stretching to 90% strain.

again. This procedure is repeated until the conductor fails. Figure 2 shows the plots of resistance $R$ vs. applied strain ε for $L = 5$ and 20 mm and $W = 95$, 45, and 25 μm, respectively. The indicated rupture strain $\varepsilon_r$ is the strain at which the resistance increases sharply. Figure 3 summarizes the rupture strain $\varepsilon_r$ of gold conductors as a function of their width $W$ and length $L$. PMDS carrying 95 μm wide conductors often tears before the conductors fail. $\varepsilon_r$ is seen to decrease with decreasing $W$ and increasing $L$. As $\varepsilon_r$ decreases the conductors become more sensitive to sample handling. For example, conductors with $W = 6$ μm have such a small $\varepsilon_r$ that they either fracture while the PDMS is peeled off its temporary glass slide carrier ($L = 20$ mm) or rupture at $\varepsilon < 2\%$ ($L = 5$ mm). Adrega et al. also observed lower yields for conductors with $W = 10$ or 20 μm than for $W > 30$ μm [10]. The macroscopic resistivity of our microcracked conductors is 7–12 times higher than the bulk resistivity of gold. The increase is caused by additional electron scattering in the thin film, by the surface roughness of the PDMS, and by the microcracks themselves. The resistivity of gold film controls deposited in the same run on a glass slide (no microcracks, low surface roughness) is 2–3 times that of bulk gold.

To understand the pronounced size dependence of the rupture strain $\varepsilon_r$ we focus on the few long cracks that form when microcracks coalesce under strain, as illustrated in Figure 4a. Such long cracks shield the surrounding microcracks from stress, because the force that drives their propagation is significantly higher than that for the microcracks. Under certain conditions, discussed below, the advance of a long crack of length $\ell$ becomes unstable, so that it runs across the entire width of the conductor ($\ell = W$) and electrical continuity is lost. Therefore the longest crack determines electrical failure. When stretched too far a conductor fails because the longest crack runs across the conductor width. We observe that such a "fatal" crack develops from a long crack that first develops in the interior of the conductor. It then continues to grow out to the edges or merges with cracks that come in from the edges. In Figure 1c the long crack in the middle is typical of those that become fatal. On the other hand, cracks that grow from the edges tend to terminate in the interior instead of running across the entire width. Such cracks can also be seen in Figure 1c. Similar observations were found for other samples. In view of this experimental evidence we model the formation of long cracks as illustrated in Figure 4b.

To quantify this mechanism we introduce a simplification that is common practice in fracture mechanics [11,12]. We approximate the conductor in Figures 1b and 4a as in Figure 4b, as having no microcracks but only the long crack in the middle and having a stiffness equivalent to that of the microcracked conductor. Crack propagation is driven by the energy release rate $G$. A crack is stable when $G$ is less than a critical value, the fracture toughness of the gold film $G_c$. When $G > G_c$ the crack propagates. Under an applied strain ε the energy release rate $G$ of the long crack in Figure 4b is [13]:

$$G = \pi E \epsilon^2 \ell \sec(\pi \ell / 2W)/2 \qquad (1)$$

where $E$ is the equivalent stiffness of gold, $\ell$ is the length of the longest crack, and $W$ is the width of the conductor. While Eq. (1) gives a good estimate of the driving force for crack propagation when $\ell \ll W$, electrical failure results from propagation of the long crack across the whole conductor, i.e. $\ell \cong W$. In this case Eq. (1) tends to overestimate $G$, given that Eq. (1) assumes no deformation of the two free edges of the conductor while in reality the free edges can deform locally to mitigate the stress concentration near the crack tips when $\ell \cong W$. Therefore, to precisely compute the driving force for crack propagation near conductor fail-

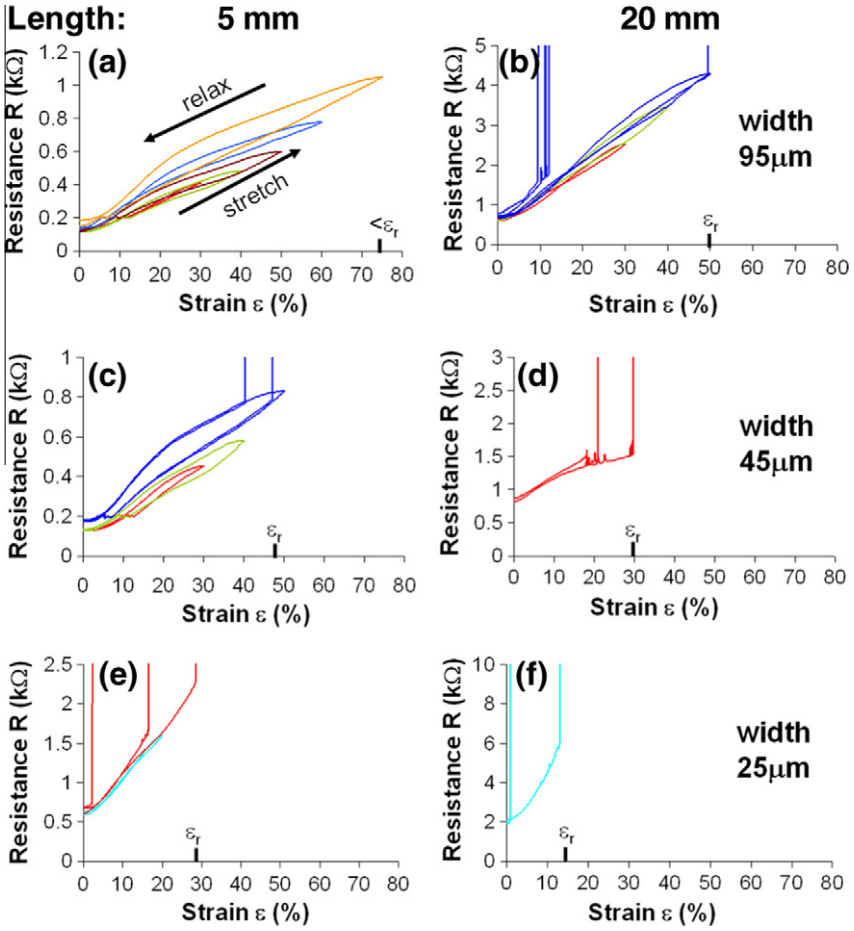


**Figure 2.** Electrical resistance $R$ measured on gold conductors as a function of applied strain. The strain rate is 0.1% every 3 s. The rupture strains $\varepsilon_r$ are marked. (a) Length $L = 5$ mm, width $W = 95$ μm; (b) $L = 20$ mm, $W = 95$ μm; (c) $L = 5$ mm, $W = 45$ μm; (d) $L = 20$ mm, $W = 45$ μm; (e) $L = 5$ mm, $W = 25$ μm; (f) $L = 20$ mm, $W = 25$ μm.

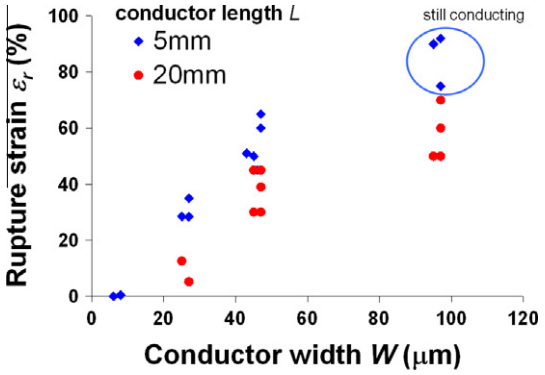


**Figure 3.** Experimentally determined rupture strain $\varepsilon_r$ as a function of width $W$ and length $L$ of gold conductors on a PDMS substrate. The ~95 μm wide conductors were still electrically conductive at the indicated strains. Mechanical failure due to tearing or slipping out of the clamp prevented determination of the exact rupture strain.

ure we simulate deformation of the gold film as in Figure 4b under remote elongation using the finite element code ABAQUS. The gold conductor is modeled as a $W \times L$ rectangular film with displacement $u$ applied to the two remote vertical edges in opposite directions to simulate the relative elongation of $\varepsilon = 2u/L$, as in Figure 4b. In the simulations, for a given conductor width $W$ (25, 45, and 95 μm, respectively) we vary the crack length $\ell$ to study its effect on the driving force for crack propagation. In the regions near two crack tips the film is densely meshed into four node quadrilateral plane stress concentric circle elements to capture the stress concentration effect. That part of the film outside these two regions is less densely meshed. The gold film is taken as a linear elastic material with a Young's modulus of 100 GPa and a Poisson's ratio of 0.3. The energy release rate $G$ can be calculated directly through the contour integral in ABAQUS [14]. Eq. (1) and a finite element method (FEM) model are applied to freestanding gold conductors without substrate, an assumption justified by the large stiffness difference between gold and PDMS of $>10^5$. Recent simulations show that under tension a patterned thin gold film on a PDMS substrate deforms almost like a freestanding thin gold film of the same pattern [15].

The results calculated from Eq. (1) and the FEM are plotted in Figure 4c as the normalized energy release rate $G/E\varepsilon^2 h$ vs. crack length $\ell$ for the conductor widths $W$ of the experiments. Here, $h$ is the thickness of the gold film. Note that $G/E\varepsilon^2 h = \pi\ell\sec(\pi\ell/2W)/2h$ depends only on geometry, not on material properties. The most important result is that the driving force for crack propagation monotonically increases with $\ell$ for any $W$. When $\ell \ll W$ the analytical solution from Eq. (1) agrees with the FEM

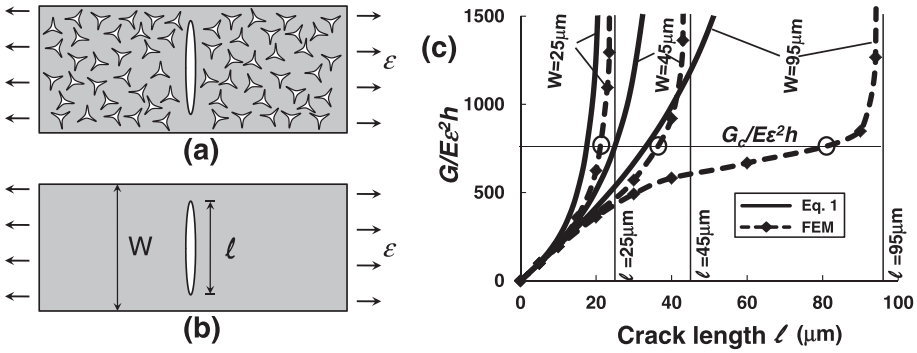


**Figure 4.** (a) When stretched, pre-existing microcracks in a metal conductor coalesce locally to form a long crack. (b) Approximation for the FEM simulation. (c) Normalized energy release rate $G/E\varepsilon^2 h$ as a function of crack length $\ell$ for conductor widths $W = 25$, 45, and 95 μm. Solid lines from Eq. (1), dashed lines from the FEM. The fracture toughness of the gold $G_c$ and the applied strain ε result in the value for $G_c/E\varepsilon^2 h$ marked by circles on the FEM curves. These identify critical crack lengths $\ell_{cr}$. For example, for $G_c/E\varepsilon^2 h = 750$ $\ell_{cr} \approx 21$, 38, and 80 μm for $W = 25$, 45, and 95 μm, respectively.

results, however, as $\ell$ approaches $W$ Eq. (1) overestimates the crack driving force compared with the FEM model, but both predict that the crack driving force approaches infinity. The critical crack length $\ell_{cr}$ demarcates the regime of stable from that of unstable crack propagation. In Figure 4c the intersections with $G_c/E\varepsilon^2 h$ of the dashed FEM curves (circles) for the normalized energy release rate $G/E\varepsilon^2 h$ determine the critical crack length $\ell_{cr}$. If the fracture toughness $G_c$ and the stiffness $E$ of the gold conductor can be determined Figure 4c can be used to correlate the critical rupture strain $\varepsilon_r$ and the corresponding critical crack length $\ell_{cr}$ for a given conductor width. For a given $G_c/E\varepsilon^2 h$, $\ell_{cr}$ increases as $W$ increases. A crack longer than $\ell_{cr}$ will propagate unstably and make the conductor fail. In other words, the wider the conductor, the longer $\ell_{cr}$, and the greater the resistance to failure. Additionally, the driving force for propagation of a crack of length $\ell$ increases with decreasing $W$. Both factors, the smaller $\ell_{cr}$ and the larger driving force for crack propagation, contribute to the decrease in rupture strain with decreasing $W$. Thus the mechanics model qualitatively explains the experimentally observed dependence of the rupture strain $\varepsilon_r$ on width $W$. The experimentally observed dependence of rupture strain $\varepsilon_r$ on conductor length $L$ can be understood from the rising probability of the formation of long microcracks with increasing $L$. Under tensile strain the probability that microcracks coalesce to a crack of length $>\ell_{cr}$ is higher for a longer conductor. This length dependence of the rupture strain is similar to the often observed size dependence of the statistical strength of brittle materials [16,17].

In summary, our experiments demonstrate that the rupture strain of a microcracked gold conductor increases with increasing width and decreasing length of the conductor. A fracture mechanics model offers a systematic account of this size dependence. When a microcracked gold conductor is stretched the microcracks coalesce and form longer cracks. The conductor remains electrically conductive provided the longest crack is shorter than a critical crack length $\ell_{cr}$. These findings highlight the importance of preventing the longest crack from exceeding $\ell_{cr}$ (e.g. by nanopatterning the silicone substrate [18]) in the design of elastically stretchable metal conductors of high deformability for use in flexible electronics. Furthermore, the mechanics model sheds light on the correlations between conductor material properties (e.g. fracture toughness), critical defect size, and conductor deformability, and provides guidance for materials selection and morphology control of stretchable metal conductors.

This research was supported by the NIH (NINDS R21 052794) and the New Jersey Commission for Science and Technology, and is supported by the New Jersey Commission on Brain Injury Research. T.L. acknowledges the support of the NSF (under Grants 0856540 and 0928278).

[1] Z. Yu, O. Graudejus, C. Tsay, S.P. Lacour, S. Wagner, B. Morrison, J. Neurotraum. 26 (2009) 1135.
[2] K.W. Meacham, R.J. Giuly, L. Guo, S. Hochman, S.P. DeWeerth, Biomed. Microdev. 10 (2008) 259.
[3] J.J. FitzGerald, S.P. Lacour, S.B. McMaho, J.W. Fawcett, IEEE Trans. Biomed. Eng. 56 (2009) 1524.
[4] R. Pelrine, R. Kornbluh, G. Kofod, Adv. Mater. 12 (2000) 1223.
[5] R. Carta, P. Jourand, B. Hermans, J. Thoné, D. Brosteaux, T. Vervust, F. Bossuyt, F. Axisa, J. Vanfleteren, R. Puers, Sens. Act A 156 (2009) 79.
[6] S.P. Lacour, J. Jones, S. Wagner, T. Li, Z. Suo, Proc. IEEE 93 (2005) 1459.
[7] O. Graudejus, P. Goerrn, S. Wagner, Appl. Mat. Int. 2 (2010) 1927.
[8] S.P. Lacour, D. Chan, S. Wagner, T. Li, Z. Suo, Appl. Phys. Lett. 88 (2006) 204103.
[9] O. Graudejus, Z. Yu, J. Jones, B. Morrison, S. Wagner, J. Electrochem. Soc. 156 (2009) 85.
[10] T. Adrega, S.P. Lacour, J. Micromech. Microeng. 20 (2010) 055025.
[11] M. Kachanov, Int. J. Solids Strut. 23 (1987) 23.
[12] S.X. Gong, H. Horii, J. Mech. Phys. Solids 37 (1989) 27.
[13] H. Tada, P.C. Paris, G.R. Irwin, The Stress Analysis of Cracks Handbook, 3rd ed., American Society of Mechanical Engineers, New York, 2000.
[14] J.R. Rice, J. Appl. Mech. Trans. ASME 35 (1968) 379.
[15] T. Li, Z. Suo, S. Lacour, S. Wagner, J. Mater. Res. 20 (2005) 3274.
[16] S. She, J.D. Landes, J.A.M. Boulet, J.E. Stoneking, J. Appl. Mech. Trans. ASME 58 (1991) 43.
[17] S.L. Zhang, T. Li, W. Yang, Int. J. Solids Struct. 35 (1998) 995.
[18] P. Mandlik, S.P. Lacour, J.W. Li, S.Y. Chou, S. Wagner, IEEE Elect. Dev. Lett. 27 (2006) 650.